*Science in China Series G: Physics, Mechanics & Astronomy*



www.scichina.com
phys.scichina.com
www.springerlink.com

# The optimal path of piston motion for Otto cycle with linear phenomenological heat transfer law

XIA ShaoJun, CHEN LinGen† & SUN FengRui

Postgraduate School, Naval University of Engineering, Wuhan 430033, China

**An Otto cycle engine with internal and external irreversibilities of friction and heat leakage, in which the heat transfer between the working fluid and the environment obeys linear phenomenological heat transfer law [$q \propto \Delta(T^{-1})$], is studied in this paper. The optimal piston motion trajectory for maximizing the work output per cycle is derived for the fixed total cycle time and fuel consumed per cycle. Optimal control theory is applied to determine the optimal piston trajectories for the cases of with and without piston acceleration constraint on each stroke and the optimal distribution of the total cycle time among the strokes. The optimal piston motion with acceleration constraint for each stroke consists of three segments, including initial maximum acceleration and final maximum deceleration boundary segments, respectively. Numerical examples for optimal configuration are provided, and the obtained results are compared with those obtained with Newton's heat transfer law [$q \propto \Delta(T)$]. The results also show that optimizing the piston motion can improve power and efficiency of the engine by more than 9%. This is primarily due to the decrease in heat leakage loss on the initial portion of the power stroke.**

linear phenomenological heat transfer law, Otto cycle, maximum work output, optimal piston trajectory, finite time thermodynamics, generalized thermodynamic optimization

There are two standard problems in finite time thermodynamics: One is to determine the objective function limits and the relations between objective functions for the given thermodynamic system, and another is to determine the optimal thermodynamic process for the given optimization objectives[1−10]. The researches on optimal configurations of thermodynamic processes include two aspects at least. The first is to study the optimal configurations of theoretical cycles and processes. Cutowicz-Krusin et al.[11] proved that in all acceptable cycles, an endoreversible Carnot cycle with larger compression ratio can produce maximum power, i.e. the Curzon-Ahlborn cycle[12] is the optimal configuration with only First and Second Law constraints. Rubin[13,14] found the optimal configurations of endoreversible heat engines with Newton's heat transfer law [$q \propto \Delta(T)$] and different constraints. The optimal configuration with fixed duration for maximum power output is a six-branch cycle, and the optimal configuration with fixed energy input for maximum efficiency is an eight-branch cycle[13]. The results are extended to a class of heat engines with fixed compression ratio, and an optimal eight-branch cycle configuration of the engines for maximum power output is derived[14]. Band et al.[15−17], Salamon et al.[18] and Aizenbud et al.[19,20] investigated the problem of maximizing the work obtained from an ideal gas inside a cylinder with a moveable piston. The gas was coupled to an external heat bath at constant temperature $T_{ex}$, and the heat transfer between the gas and bath obeyed Newton's heat transfer law [$q \propto \Delta(T)$]. Huleihil et al.[21] considered optimal piston motion derived for adiabatic process in the presence of different types of friction, and found that in the externally dissipative mode maximiz-

Received July 4, 2008; accepted December 8, 2008
doi: 10.1007/s11433-009-0091-4
†Corresponding author (email: lgchenna@yahoo.com, lingenchen@hotmail.com)
Supported by the Program for New Century Excellent Talents in University of China (Grant No. 20041006) and the Foundation for the Author of National Excellent Doctoral Dissertation of China (Grant No. 200136)

ing power or minimizing frictional loss are equivalent, while in the internally dissipative mode the optimal motions are different for the two optimization objectives. The second is to study the optimal paths of piston motion for practical engines. Mozurkewich and Berry[22,23] investigated a four stroke Otto cycle engine with losses of piston friction and heat leakage, in which the heat transfer between the working fluid and the cylinder wall obeys Newton's heat transfer law $[q \propto \Delta(T)]$. The optimal piston trajectory for maximizing the work output per cycle was derived for the fixed total cycle time and fuel consumed per cycle. It turned out that optimizing the piston motion could improve engine efficiency by nearly 10%. Hoffman et al.[24] and Blaudeck and Hoffman[25] further considered the effect of the finite combustion rate of the fuel on the performance of engines, and studied the optimal piston motion for a four-stroke Diesel cycle engine with losses of piston friction and heat leakage, in which the heat transfer between the working fluid and the cylinder wall also obeys the Newton's heat transfer law $[q \propto \Delta(T)]$. In general, heat transfer is not necessarily Newton's heat transfer law and also obeys other laws; heat transfer laws not only have significant influences on the performance of the given thermodynamic process[26−32], but also have influences on the optimal configurations of thermodynamic process for the given optimization objectives. Song et al.[33−35] determined the optimal configurations of endoreversible heat engines for maximum efficiency objective and maximum power output objective with linear phenomenological heat transfer law $[q \propto \Delta(T^{-1})]$[33] and those for maximum power output with fixed duration and radiative heat transfer law $[q \propto \Delta(T^4)]$[34,35], and derived the results different from those obtained by Rubin[13]. Chen et al.[36] and Song et al.[37] determined the optimal configurations of expansion process of a heated working fluid in the piston cylinder with linear phenomenological $[q \propto \Delta(T^{-1})]$[36] and generalized radiative $[q \propto \Delta(T^n)]$[37] heat transfer laws. Burzler and Hoffman[38] and Burzler[39] considered the effects of convective-radiative heat transfer law $[q \propto \Delta(T) + \Delta(T^4)]$ and non-ideal working fluid, and derived the optimal piston motion for maximizing power output during the compression and power strokes of a four stroke Diesel engine. Based on refs. [22,23], this work studies the optimal piston trajectory of the Otto cycle engine for maximizing work output per cycle with the fixed total cycle time, the fixed fuel consumed per cycle and linear phenomenological heat transfer law $[q \propto \Delta(T^{-1})]$ in the heat transfer process between working fluid and the environment. Numerical examples for optimal configurations are provided, and the obtained results are compared with those obtained with the Newton's heat transfer law $[q \propto \Delta(T)]$[22,23]. The research on the optimal configurations of the engines from Newton's heat transfer law to linear phenomenological heat transfer law enriches the finite time thermodynamic theory. The results presented herein can provide guidelines for optimal design and operation of real internal combustion engines.

## 1 The Otto cycle engine model

A four-stroke Otto cycle engine model is studied in this paper. The effects of the finite combustion rate of the fuel during the power stroke on the performance of the engine are not considered here, and the fuel combustion process is completed instantaneously. The fixed fuel consumed per cycle is equivalent to the given initial working fluid temperature on the power stroke. The working fluid in the cylinder is assumed to consist of an ideal gas which is in internal equilibrium all the time. Besides, according to refs. [22−25,40,41], the major losses in real internal combustion engines and the piston motion of the conventional engine are simplified and described qualitatively and quantitatively below.

### 1.1 Heat leakage

In real internal combustion engine, power loss due to heat transfer from the working fluid to the environment outside the cylinder typically costs about 12% of the power produced by the engine. Different from refs. [22−25] with the Newton's heat transfer law $[q \propto \Delta(T)]$, the heat transfer between the working fluid and the environment outside the cylinder is assumed to obey the linear phenomenological heat transfer law $[q \propto \Delta(T^{-1})]$. The heat transfer expression used here assumes that the rate is linear in the inside surface area of the cylinder and in the difference of reciprocal temperatures between the temperature $T$ of the working fluid and that of the wall $T_w$. $T_w$ is assumed to be a constant. For heat transfer coefficient $k$ and cylinder inner diameter $b$, the rate of

heat leakage at position $X$ (see Figure 1) is

$$\dot{Q} = k\pi b(b/2 + X)(T_{\mathrm{w}}^{-1} - T^{-1}). \quad (1)$$

The effect of heat transfer is only important on the power stroke. The rate is negligible on the other strokes.

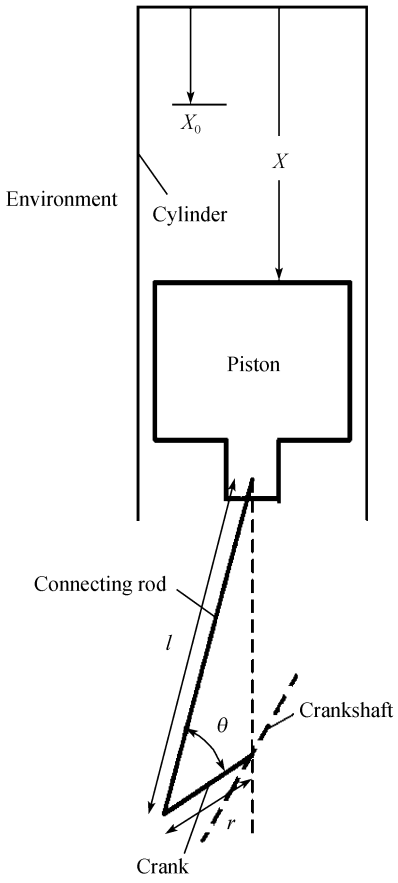


**Figure 1** Conventional piston linkage.

### 1.2 Other losses[22,23]

In real internal combustion engine, friction typically dissipates about 20% of the total power produced by the engine. Of which about 75% is due to the friction of the piston rings on the cylinder walls and 25% is in the crankshaft bearings[40]. The former contribution is considered in this paper, while the latter one is negligible. If $W_{\mathrm{R}}$ is the reversible work per cycle and $W_{f,\tau}$ is the total work loss per cycle due to friction loss, one has $W_{f,\tau} = 0.15W_{\mathrm{R}}$. The viscosity of the working fluid is neglected and a friction force $f$ is assumed to be linear in velocity $v$, i.e. $f = \mu v$, where $\mu$ is the friction coefficient of the compression and exhaust strokes. The friction coefficient on the power stroke is assumed to be $2\mu$, which is due to greater pressure on the upside of the piston. For the intake stroke, when the gas flows through the inlet valve, there is an additional friction-like loss term, which is due to the pressure differential caused by viscosity[40]. The pressure differential is proportional to velocity, so it may be included in the friction term for the intake stroke, and then the friction coefficient on the intake stroke is assumed to be $3\mu$. Besides, there are effects of the time losses due to beginning the expansion stroke while combustion is still taking place and the exhaust blowdown due to opening the exhaust valve before completion of the expansion stroke. They are so small compared with the heat leakage and friction losses that they are all negligible.

### 1.3 Piston motion of a conventional engine[41]

Figure 1 shows a typical piston to crankshaft linkage, where $X_0$ is the initial position of the piston on the power stroke, $l$ is the length of connecting rod, $r$ is the length of brace, and $\theta$ is the rotating angle of crankshaft. With the analysis of the geometrical relationships among different components, the equation of motion for the piston is

$$v = \dot{X} = (2\pi\Delta X/\tau)(\sin\theta) \times \{1 + r\cos\theta[1 - (r/l)^2\sin^2\theta]/l\}^{-1/2}, \quad (2)$$

where $\theta = 4\pi t/\tau$ and $\Delta X = 2r$. If $X_{\mathrm{f}}$ is the final position of the piston on the power stroke, $X_f = X_0 + 2r$. $\tau$ is the total cycle time (two crankshaft revolutions). $X = X_0$ when $t = 0$. If $r/l = 0$ the motion would be purely sinusoidal.

## 2 The optimization procedure

The optimization problem is maximizing the work per cycle for fixed fuel consumption and total cycle time. Thus the only difference between the optimized engine and the conventional one is in the piston motion. Because the total cycle time and fuel consumed per cycle are fixed, maximizing work per cycle, efficiency and average power are all identical. The optimization procedure consists of two parts. The first is to determine the optimal trajectory on each stroke as a function of the time spent on that stroke. The second is to optimize the distribution of the total cycle time among the strokes. A real engine includes power and nonpower strokes. Nonpower strokes include intake, compression and exhaust strokes, all of which waste power produced on the power stroke and have no heat leakage. Therefore, the optimization of these strokes is relatively simple, and the

three strokes can be treated together to simplify the optimization problem. Thus the optimization procedure consists of nonpower stroke and power stroke optimizations. For the three nonpower strokes, at first, the piston path on each stroke is determined with the objective of minimum frictional loss, respectively, and then the time allocation among three non-power strokes for a fixed total time $t_{\rm np}$ is determined with the objective of minimum total frictional losses $W_{f,t_{\rm np}}$, while for the power stroke, the piston path is determined with the objective of maximum work output $W_P$ per stroke. For the total cycle, the distribution of the total cycle time $\tau$ between the total time $t_{\rm np}$ of nonpower strokes and the power stroke time $t_p$ is determined with the objective of maximum work $W_\tau$ per cycle.

### 2.1 Optimization for nonpower strokes

First is to determine the optimal path for minimizing frictional loss on a single nonpower stroke. For a single stroke completed in time $t_1$, the work loss due to friction is

$$W_{f,t_1} = \int_0^{t_1} \mu v^2 \mathrm{d}t. \tag{3}$$

According to the results in refs. [22—25], when there is no constraint on the acceleration, the optimal piston motion of a single nonpower stroke is that the velocity of the piston during the total stroke is a constant, which is equivalent to the ratio of the stroke length $\Delta X$ to the time $t_1$ spent on that stroke. For the case in which the acceleration is constrained to lie between $-a_{\rm m}$ and $a_{\rm m}$, the optimal trajectory is as follows: Start at $v=0$, accelerate at the maximum rate until some time $t_a$, run at constant velocity $v=a_{\rm m}t_a$ until $t_1-t_a$, then decelerate at the maximum rate for the rest of the stroke until $v=0$. For the optimal piston motion on nonpower strokes with constraint on the acceleration, the time $t_a$ and the work loss $W_{f,t_1}$ due to friction are obtained as follows. Note that the piston moves a distance $\Delta X$ in time $t_1$, one has

$$\Delta X = a_m t_a^2 + a_m t_a (t_1 - 2t_a). \tag{4}$$

Solving $t_a$ gives

$$t_a = t_1(1-y_1)/2, \tag{5}$$

where $y_1 = (1-4\Delta X/a_m t_1^{\,2})^{1/2}$. The work loss due to friction per stroke is obtained by integrating eq. (3):

$$W_{f,t_1} = \mu[2\int_0^{t_a}(a_m t)^2 \mathrm{d}t + \int_{t_a}^{t_1-t_a}(a_m t_a)^2 \mathrm{d}t]. \tag{6}$$

Substituting eq. (5) into eq. (6) yields

$$W_{f,t_1} = \mu a_m{}^2 t_1{}^3 (1+2y_1)(1-y_1)^2/12. \tag{7}$$

Second is to determine the optimal allocation of the total time $t_{\rm np}$ among the three nonpower strokes for minimizing the total work loss $W_{f,t_{\rm np}}$ due to friction. The friction coefficient $\mu$ is the same on the exhaust and compression strokes. Therefore the time $t_1$ spent on each of these strokes is the same. The friction coefficient on the intake stroke is $3\mu$, and let the time spent on this stroke be $t_2$. Thus the total time for the three strokes is $t_{\rm np} = 2t_1 + t_2$. Using eq. (7), the total work loss due to friction on the nonpower strokes is

$$W_{f,t_{\rm np}} = \mu a_{\rm m}^2 \frac{2t_1^3(1-y_1)^2(1+2y_1) + 3t_2^3(1-y_2)^2(1+2y_2)}{12}. \tag{8}$$

From the extremum condition $\partial W_{f,t_{\rm np}}/\partial t_2 = 0$, one obtains

$$t_1^2(1-y_1)^2 = 3t_2^2(1-y_2)^2. \tag{9}$$

For a given value of $t_{\rm np}$, eq. (9) can be solved numerically to get $t_1$ and $t_2$.

For the case without constraint on acceleration, i.e. $a_m \to \infty$, eq. (9) becomes

$$t_2 = \sqrt{3}t_1. \tag{10}$$

And the total frictional loss, from eq. (8), is

$$W_{f,t_{\rm np}} = \mu(2+\sqrt{3})^2(\Delta X)^2/t_{\rm np}. \tag{11}$$

### 2.2 Optimization for power stroke

For the power stroke, the problem is to optimize the piston motion with the objective of maximum work $W_P$ per stroke, i.e. to determine the optimal relationship between $W_P$ and $t_P$. Different from the optimization of the nonpower strokes, in which we only consider the friction loss, the optimization of the power stroke also considers the effects of heat leakage on the optimal piston trajectory. It's difficult to solve for the optimal piston motion with acceleration constraint directly, so a problem without constraints either on the acceleration or on the time to complete the power stroke is solved firstly. The solution of this problem provides reasonable initial values for solving the problem with acceleration constraint[22,23].

2.2.1 Power stroke with unconstrained time. For the

case without time constraint, if the problem is parametrized in terms of the piston position $X$ rather than the time $t$, it is no longer necessary to specify a time duration for the power stroke. The working fluid is assumed to be an ideal gas. In terms of the first law of thermodynamics, one has

$$\mathrm{d}T/\mathrm{d}X = -\frac{NRTv + k\pi bX(b/2+X)(T_{\mathrm{w}}^{-1} - T^{-1})}{NCXv}, \quad (12)$$

where $N$ is the number of moles of the working fluid, $R$ is gas constant, and $C$ is the heat capacity of the working fluid. In order to get the maximum work output during the power stroke, the optimization problem becomes

$$\max\ W_p = \int_{X_0}^{X_{\mathrm{f}}} (NRT/X - 2\mu v)\mathrm{d}X. \quad (13)$$

The Hamiltonian is

$$H = NRT/X - 2\mu v - \lambda[NRTv + k\pi bX(b/2+X) \times (T_{\mathrm{w}}^{-1} - T^{-1})]/(NCXv). \quad (14)$$

The canonical equations are eq. (12) and

$$\mathrm{d}\lambda/\mathrm{d}X = -\partial H/\partial T = NR/X - \lambda R/(CX) + \lambda k\pi b(b/2+X)/(NCvT^2). \quad (15)$$

From the extremum condition $\partial H/\partial v = 0$, one has

$$v = [k\pi b\lambda(T_{\mathrm{w}}^{-1} - T^{-1})(b/2+X)/(2\mu CN)]^{1/2}. \quad (16)$$

In solving these equations, there are two boundary conditions to be satisfied. They are

$$T(X_0) = T_0,\ \ \lambda(X_{\mathrm{f}}) = 0. \quad (17)$$

The above equations have no closed-form solution, which need to be solved numerically. An initial value of $\lambda(X_0)$ is guessed, and then eqs. (12), (15) and (16) are solved numerically, and the value of $\lambda(X_0)$ is altered iteratively until $\lambda(X_{\mathrm{f}}) = 0$.

2.2.2 Power stroke with unconstrained acceleration. For the case with unconstrained acceleration, the value of acceleration could be arbitrary, i.e., the velocity could change instantaneously. Therefore it is unnecessary to constrain the piston velocity on two endpoints of the power stroke. The optimization problem becomes to determine the optimal path of piston motion for maximizing the work $W_p$ on the power stroke in time $t_p$. This is given by

$$\max\ \ W_p = \int_0^{t_p} (NRT\dot{X}/X - 2\mu\dot{X}^2)\,\mathrm{d}t \quad (18)$$

with the constraint

$$\dot{T} = -[NRT\dot{X}/X + k\pi b(b/2+X)(T_{\mathrm{w}}^{-1} - T^{-1})]/(NC), \quad (19)$$

where $\dot{T} = \mathrm{d}T/\mathrm{d}t$, one point above a parameter denotes the time derivative of the parameter. For the optimal control problem with constraint of differential eq. (19), the Lagrangian is

$$L = NRT\dot{X}/X - 2\mu\dot{X}^2 + \lambda[\dot{T} + RT\dot{X}/(CX) + k\pi b(b/2+X)(T_w^{-1} - T^{-1})/(NC)], \quad (20)$$

where $\lambda$ is a Lagrange multiplier. The Euler-Lagrange equations to determine the optimal path are

$$\partial L/\partial X - \mathrm{d}(\partial L/\partial\dot{X})/\mathrm{d}t = 0, \quad (21)$$

$$\partial L/\partial T - \mathrm{d}(\partial L/\partial\dot{T})/\mathrm{d}t = 0. \quad (22)$$

Substituting eq. (20) into eqs. (21) and (22), respectively, yields

$$4\mu\ddot{X} - NR\dot{T}/X - \lambda R\dot{T}/(CX) - \dot{\lambda}RT/(CX) + \lambda k\pi b(T_{\mathrm{w}}^{-1} - T^{-1})/(NC) = 0, \quad (23)$$

$$\dot{\lambda} = \frac{NR\dot{X}}{X} + \frac{\lambda R\dot{X}}{CX} + \frac{\lambda k\pi b(b/2+X)}{NCT^2}. \quad (24)$$

A system of differential equations can be obtained by using eqs. (19), (23) and (24):

$$\dot{X} = v, \quad (25)$$

$$\dot{v} = -k\pi b\{NR(T_{\mathrm{w}}^{-1} - T^{-1})(b/2+X)/X + \lambda(RT_{\mathrm{w}}^{-1} - 2T^{-1})(b/2+X)/(CX) + (T_{\mathrm{w}}^{-1} - T^{-1})\}/(4\mu NC), \quad (26)$$

$$\dot{\lambda} = Rv(NC+\lambda)/(CX) + \lambda k\pi b(b/2+X)/(NCT^2). \quad (27)$$

In solving these equations, there are four boundary conditions to be satisfied. They are

$$X(0) = X_0,\ \ X(t_p) = X_{\mathrm{f}},\quad T(0) = T_0,\ \ \partial L/\partial T|_{t=t_p} = \lambda(t_p) = 0, \quad (28)$$

where $T_0$ is the initial temperature of working fluid on the power stroke. Eqs. (19), (25)—(27) determine the optimal solution of the problem, which could be solved for the maximum value of $W_p$ as a function of $t_p$ and the optimal path of piston motion, i.e. optimal relationship between piston velocity $v$ and position $X$. The total nonpower stroke time $t_{\mathrm{np}}$ could be derived by substituting the optimal value of $t_p$ into the total cycle time $\tau = t_{\mathrm{np}} + t_p$. Then the optimal distribution of the time $t_{\mathrm{np}}$ among the three nonpower strokes and the optimal path of the piston motion on each nonpower stroke could also be determined by solving eq. (9) numerically. The system of eqs. (19), (25)—(27) have no analytical solu-

tion, which need to be solved numerically. For the details in calculations, see sec. 3.2.

2.2.3 Power stroke with constrained acceleration. For the case with constrained acceleration, the piston velocity is required to be zero at both end points and the acceleration is constrained to lie within finite limits. The optimization objective is to maximize the function given by eq. (18), the differential constraints on the state variables $T$ and $X$ remain as given in eqs. (19) and (25), respectively. Besides, the dependence of the state variable $v$ on the control variable $a$ and the inequality constraints on variable $a$ are given by

$$\dot{v} = a, \tag{29}$$

$$-a_{\mathrm{m}} \leqslant a \leqslant a_{\mathrm{m}}. \tag{30}$$

Compared with the case without acceleration constraint, the case with constrained acceleration has an additional inequality constraint eq. (30). The Hamiltonian for this problem is

$$H = NRTv / X - 2\mu v^2 - \lambda_1[NRTv + k\pi bX(b/2 + X) \times (T_{\mathrm{w}}^{-1} - T^{-1})]/(NCX) + \lambda_2 v + \lambda_3 a. \tag{31}$$

The canonical equations conjugate to eqs. (19), (25) and (29) are

$$\dot{\lambda}_1 = -\partial H / \partial T = Rv(\lambda_1 - NC)/(CX) + \lambda_1 k\pi b(b/2 + X)/(NCT^2), \tag{32}$$

$$\dot{\lambda}_2 = -\partial H / \partial X = Rv(NC - \lambda_1)/(CX^2) + \lambda_1 k\pi b(b/2 + X)(T_{\mathrm{w}}^{-1} - T^{-1})/(NC), \tag{33}$$

$$\dot{\lambda}_3 = -\partial H / \partial v = 4\mu v - \lambda_2 - RT(NC - \lambda_1)/(CX). \tag{34}$$

From the maximum principle, the condition for an interior maximum is $\partial H / \partial a = 0$, one has

$$\lambda_3 = 0. \tag{35}$$

If eq. (35) holds for more than isolated points between $-a_{\mathrm{m}}$ and $a_{\mathrm{m}}$, one also has

$$\dot{\lambda}_3 = 0. \tag{36}$$

Eliminating $\lambda_2$ by using eqs. (33), (34) and (36), the same set of differential equations as that obtained for the case of without acceleration constraint is obtained. On this basis one can conclude that the optimal trajectory with acceleration constraint on the power stroke is a three-branch path, i.e. two boundary segments (maximum acceleration and maximum deceleration) connected by a segment which satisfies the system of eqs. (19) and (25)—(27). For these equations, only numerical results could be obtained. For the details in the calculations, see sec. 3.3.

## 3 Numerical examples and discussion

### 3.1 Determination of the related constants and parameters

According to refs. [22,23,40,41], the following parameters are used in the calculations: the initial piston position on the power stroke $X_0 = 1$ cm, the final piston position on the power stroke $X_{\mathrm{f}} = 8$ cm, the length of a single stroke $\Delta X = 7$ cm, the cylinder diameter $b = 7.98$ cm, the cylinder volume $V = 400$ cm$^3$, the cycle time $\tau = 33.3$ ms corresponding to the rotating speed $n = 3600$ r/min, gas constant $R = 8.314$ J/(mol·K); the initial temperature, the number of moles and constant volume heat capacity of working fluid on the power stroke are $T_{0P} = 2795$ K, $N_P = 0.0157$ mol and $C_{vP} = 3.35R$, respectively, while on the compression stroke, the corresponding values are $T_{0\mathrm{C}} = 333$ K, $N_{\mathrm{C}} = 0.0144$ mol and $C_{v\mathrm{C}} = 2.5R$, respectively; the constant temperature of the environment outside cylinder $T_{\mathrm{w}} = 600$ K. For a conventional engine, typically $r/l$ in eq. (2) is between 0.16 and 0.40[41]; $r/l = 0.25$ is chosen for these calculations. Varying the value of $r/l$ has little effect on the results. For a reversible Otto cycle, the reversible work ouput per cycle $W_{\mathrm{R}}$ is given by

$$W_{\mathrm{R}} = N_P C_{vP} T_{0P}[1 - (X_0 / X_{\mathrm{f}})^{R/C_{vP}}] + N_{\mathrm{C}} C_{v\mathrm{C}} T_{0\mathrm{C}}[1 - (X_{\mathrm{f}} / X_0)^{R/C_{v\mathrm{C}}}]. \tag{37}$$

The result is $W_{\mathrm{R}} = 435.9$ J. Besides these parameters, the values of the friction coefficient $\mu$ and the heat transfer coefficient $k$ should also be determined for numerical calculations.

The friction coefficient $\mu$ is determined according to the pure sinusoidal piston motion[22−25]. Set $r/l = 0$ in eq. (2), the equation of motion is derived. The time spent on each stroke is $\tau/4$. Integrating eq. (3) from 0 to $\tau/4$ gives the friction loss for one stroke:

$$W_{f,\tau/4} = [\mu\pi^2(\Delta X)^2]/(2\tau). \tag{38}$$

Now if the friction coefficients of the intake, compression, power and exhaust strokes are $3\mu$, $\mu$, $2\mu$ and $\mu$, respectively, the frictional loss for the full cycle is

$$W_{f,\tau} = [7\mu\pi^2(\Delta X)^2]/(2\tau). \tag{39}$$

From the model hypothesis of $W_{f,\tau} = 0.15W_{\mathrm{R}}$, one obtains $\mu = 12.9$ kg/s.

The heat transfer coefficient $k$ is determined by a

trial-and-error method. Letting $\bar{Q}$ and $\bar{\eta}$ be the average rate of heat leakage and thermal efficiency (first-law efficiency), one has the work lost due to the heat leakage:

$$W_Q \approx \bar{\eta}\bar{Q}\tau/4. \tag{40}$$

From eq. (1), one has

$$\bar{Q} \approx k(b/2+\bar{X})(\pi b)(T_W^{-1}-\bar{T}^{-1}). \tag{41}$$

Let the average distance of piston movement and the average temperature of working fluid be $\bar{X}=4.5$ cm and $\bar{T}=1800$ K. According to ref. [40], $\bar{\eta}=0.157$. From the model hypothesis, $W_Q/W_R=0.1$ is chosen. Using eqs. (40) and (41), one has $k=1.41\times10^9$ W·K/m$^2$.

In the following results of numerical calculations, $v_{max}$ is the maximum piston velocity on the power stroke, $T_f$ is the final temperature of working fluid on the power stroke, $\varepsilon$ is the effectiveness, i.e. the second-law efficiency[42].

### 3.2 Numerical examples for the case with unconstrained acceleration

From the results for the optimal trajectory with unconstrained time on the power stroke, the reasonable initial values of piston velocity $v_0$ and acceleration $a_0$ for the optimal trajectory with unconstrained acceleration are obtained. Substituting the initial value of the acceleration $a_0$ into eq. (26) yields the initial value of $\lambda_0$. Eqs. (19) and (25)—(27) are then solved numerically until the final boundary conditions of eq. (28) are met. One value of $t_p$ is obtained. Parameter $t_p$ may be a large value, then solutions for shorter $t_p$ are obtained by increasing $v_0$. Repeating the above calculational process until $t_p<\tau$ and the maximum $W_\tau$ is obtained.

Table 1 lists some parameters (other parameters are unchanged) for various cases with unconstrained acceleration. Table 2 lists the calculational results for the corresponding cases, where the modified sinusoidal motion ($r/l=0.25$) is chosen as the conventional motion. From Table 2, one can see the influences of different choices of friction coefficient, heat leak coefficient and cycle time on the optimal configurations of piston movement. For different cases, the results in Table 2 show that the peak velocity with the optimal piston motion is much larger than that with the conventional motion, respectively. The peak velocity appears on the power stroke, so the friction loss on this stroke with the optimal piston motion may be larger than that with the conventional motion. However, an increase in the average velocity on the power stroke results in a decrease in time $t_p$. Thus on the one hand, the heat leakage loss is decreased for the decrease in the time spent on the contact between the high-temperature working fluid and the environment outside the cylinder. On the other hand, the average velocities on the nonpower strokes are decreased for increases in the times spent on these strokes, this decreases the friction losses on the nonpower strokes. The amount of decrease in the total friction losses on the nonpower strokes is always larger than the amount of the increase in the frictional loss on the power stroke, so the total frictional loss per cycle $W_{f,\tau}$ is decreased. Both the heat leakage loss $Q$ and the frictional loss $W_{f,\tau}$ are decreased, the work per cycle $W_\tau$ and the effectiveness $\varepsilon$ with the optimal piston motion are larger than those with the conventional piston motion. The numerical results are summarized in Table 2.

**Table 1** Parameters for different cases with unconstrained acceleration

| Case | $\mu$ (kg/s) | $k$ ($\times10^9$ W·K/m$^2$) | $\tau$ (ms) | $n$ (r/min) |
|---|---|---|---|---|
| (1) | 12.9 | 1.41 | 33.33 | 3600 |
| (2) | 7.5 | 2.50 | 33.33 | 3600 |
| (3) | 17.2 | 0.80 | 33.33 | 3600 |
| (4) | 12.9 | 1.41 | 25.00 | 4800 |
| (5) | 12.9 | 1.41 | 50.00 | 2400 |

**Table 2** Numerical results for different cases with unconstrained acceleration

| Case | | $v_{max}$ (m/s) | $t_p$ (ms) | $W_p$ (J) | $W_\tau$ (J) | $W_{f,\tau}$ (J) | $W_Q$ (J) | $Q$ (J) | $W_Q/Q$ | $T_f$ (K) | $\varepsilon$ |
|---|---|---|---|---|---|---|---|---|---|---|---|
| (1) | conv. | 13.3 | 8.33 | 504 | 285 | 66.6 | 41.8 | 242 | 0.173 | 1044 | 0.654 |
| | opt. | 20.4 | 5.18 | 516 | 317 | 57.9 | 22.7 | 165 | 0.138 | 1176 | 0.727 |
| (2) | conv. | 13.3 | 8.33 | 481 | 282 | 38.7 | 72.7 | 378 | 0.192 | 804 | 0.647 |
| | opt. | 35.6 | 2.92 | 515 | 330 | 43.7 | 23.4 | 167 | 0.140 | 1172 | 0.758 |
| (3) | conv. | 13.3 | 8.33 | 516 | 281 | 88.8 | 23.5 | 146 | 0.161 | 1224 | 0.646 |
| | opt. | 13.2 | 8.09 | 523 | 308 | 69.6 | 19.9 | 147 | 0.135 | 1210 | 0.706 |
| (4) | conv. | 17.7 | 6.25 | 509 | 274 | 88.7 | 31.3 | 188 | 0.166 | 1144 | 0.628 |
| | opt. | 21.9 | 4.96 | 516 | 304 | 71.6 | 21.6 | 161 | 0.134 | 1183 | 0.698 |
| (5) | conv. | 8.86 | 12.5 | 490 | 287 | 44.3 | 62.2 | 336 | 0.185 | 876 | 0.659 |
| | opt. | 19.3 | 6.68 | 517 | 328 | 43.0 | 25.6 | 214 | 0.120 | 1176 | 0.754 |

### 3.3 Numerical examples for the case with constrained acceleration

The optimal trajectory with constrained acceleration on the power stroke is a three-branch path. In contrast to the forward numerical calculation for the case with unconstrained acceleration, the system of differential equations for the case with constrained acceleration is solved backwards.

The first is to calculate the maximum deceleration segment. The value of the final temperature $T_f$ on the power stroke is guessed, meanwhile, the time spent on the maximum deceleration segment is chosen, then solve for the initial various parameters on this segment. The second is to calculate the interior segment. Using the calculational results of the former step as the initial values of this step, one can solve the differential equations backwards with the Runge-kutta method. The piston velocity on the initial position of the interior segment is related to the piston position, which could be a switching point from the interior segment to the maximum acceleration segment. The third is to calculate the maximum acceleration segment. Using the calculated results of the former step as the initial values of this step, one can solve backwards for the initial temperature $T_{0P}$. The resulting value of $T_{0P}$ is compared with the desired one. The guessed initial value of $T_f$ is then modified to minimize the square of the deviation between the resulting value and the desired value of $T_{0P}$, and the work per cycle $W_\tau$ is solved. The fourth is to modify the value of the time spent on the maximum deceleration segment, and to repeat the former three steps until all of the values of the time spent on the maximum deceleration segment are calculated. The fifth is to compare the work output per cycle $W_\tau$ with different values of time spent on the maximum deceleration segment and to select the maximum $W_\tau$.

For the constrained acceleration cases, the lower limit of the acceleration corresponds roughly to the maximum acceleration in the conventional motion, while the upper limit is roughly chosen according to the optimal trajectory with constrained acceleration[23]. In the calculations, $a_{max}$ is varied from $5\times10^3$ to $5\times10^4$ m/s$^2$, the friction coefficient is $\mu=12.9$ kg/s, the heat transfer coefficient is $k=1.41\times10^9$ W·K/m$^2$, and the total cycle time is $\tau=33.3$ ms. Table 3 lists the results for the constrained acceleration calculations. Figure 2 shows the optimal configuration of piston motion on the power stroke for different values of the maximum acceleration. From Figure 2, one can see that the interior segment of the optimal trajectory for maximum acceleration of $5\times10^4$ m/s$^2$ is very similar to that for unconstrained acceleration case, this is because they satisfy the same system of differential equations with different boundary conditions. But they are different in the initial and final segments of piston motion on the power stroke. The optimal piston motion with $a_{max}=5\times10^4$ m/s$^2$ must compensate for the time lost on the initial maximum acceleration and final maximum deceleration segments (the velocity is zero at both end points), while for the case with unconstrained acceleration, the maximum acceleration limit could be an infinite value, then the velocity could change instantaneously.

Figure 3 shows the various piston motions on the power stroke with different constraints, which includes the conventional motion, the optimal trajectory for maximum acceleration of $5\times10^3$ m/s$^2$ and the symmetric case. This last case is one for which the trajectory is required to be the same on all four strokes, and the value of maximum acceleration is $1\times10^4$ m/s$^2$. From Figure 3, compared with the conventional motion, the peak velocity on the power stroke for the symmetric case is higher and much closer to the beginning of the power stroke, the heat leakage is decreased as a result of the decrease in the time spent on heat exchange between the working fluid and the environment outside the cylinder during the initial high-temperature segment. This is concluded from the changes of the heat leakage $Q$. Compared with the conventional motion, the work per cycle $W_\tau$ and the effectiveness $\varepsilon$ for the symmetric case are also improved.

**Table 3** Numerical results for optimal trajectories with different values of constrained acceleration

| Case | | $v_{max}$ (m/s) | $t_p$ (ms) | $W_p$ (J) | $W_\tau$ (J) | $W_{f,\tau}$ (J) | $W_Q$ (J) | $Q$ (J) | $W_Q/Q$ | $T_f$ (K) | $\varepsilon$ |
|---|---|---|---|---|---|---|---|---|---|---|---|
| Conventional | | 13.3 | 8.33 | 504 | 285 | 66.6 | 41.8 | 242 | 0.173 | 1044 | 0.654 |
| Constrained acceleration $a_{max}$ (m/s$^2$) | $5\times10^3$ | 18.4 | 7.61 | 504 | 286 | 63.7 | 43.4 | 223 | 0.179 | 1100 | 0.656 |
| | $1\times10^4$ | 19.9 | 5.94 | 509 | 292 | 58.6 | 33.6 | 199 | 0.139 | 1110 | 0.670 |
| | $2\times10^4$ | 20.5 | 5.33 | 512 | 298 | 58.4 | 29.3 | 186 | 0.121 | 1107 | 0.684 |
| | $5\times10^4$ | 19.9 | 5.87 | 513 | 311 | 58.5 | 26.6 | 177 | 0.110 | 1142 | 0.714 |
| Unconstrained acceleration | | 20.4 | 5.18 | 516 | 317 | 57.9 | 22.7 | 165 | 0.094 | 1176 | 0.727 |
| Symmetric | | 17.4 | 8.32 | 507 | 289 | 58.6 | 39.7 | 205 | 0.164 | 1104 | 0.663 |

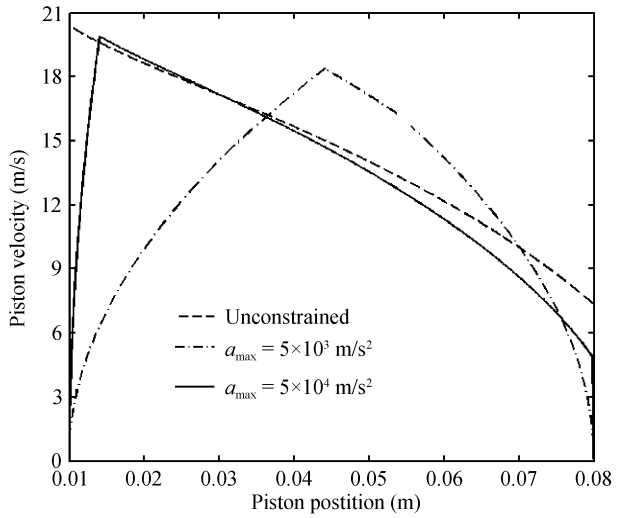


**Figure 2** Optimal trajectories for various maximum accelerations.

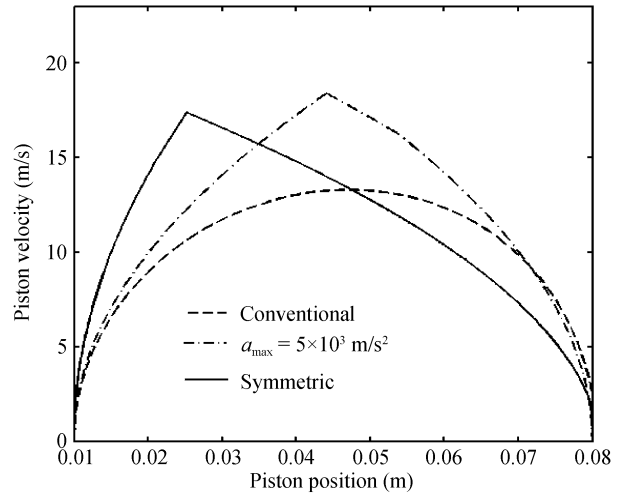


**Figure 3** Comparison of conventional, symmetric, and optimized trajectories.

Compared with the optimal piston motion with the maximum acceleration $5\times10^3$ m/s$^2$, the total friction loss for the symmetric case could also be decreased for the uniform distribution of the velocity on each stroke. Table 3 shows that $W_{f,\tau}$ is decreased remarkably. Figure 4 shows the optimal configuration of the piston motion for the whole cycle with the maximum acceleration limit $a_{max} = 5\times10^4$ m/s$^2$.

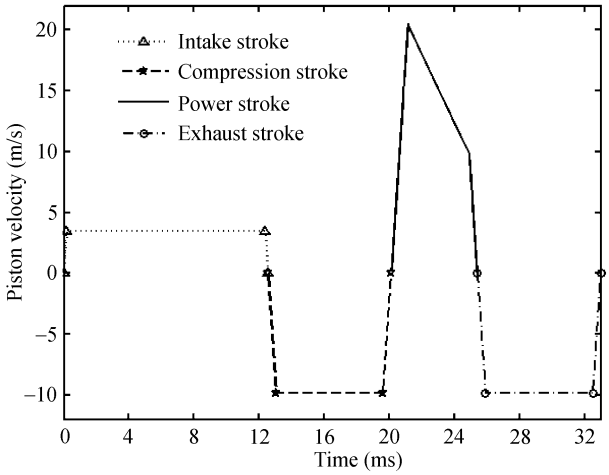


**Figure 4** Optimal trajectory for the full cycle with $a_{max} = 2\times10^4$ m/s$^2$.

### 3.4 Comparison between the optimal and conventional piston motions

Table 4 lists the comparison results between the optimal trajectory and the conventional motion for different cases. It shows that whether with or without constrained acceleration cases, both $W_Q$ and $Q$ are decreased after optimizing the piston motion, and the optimization has a much more pronounced effect on $W_Q$ than on $Q$. The reasons include two major respects. First, the heat leakage loss mainly occurs on the power stroke, and the time spent on the power stoke is decreased after optimizing the piston motion, i.e. the time spent on the contact between the working fluid and the cylinder wall is decreased, then the heat leakage loss is decreased. Second, the main portion of the heat leakage loss lies at the beginning of the power stroke (high temperature), and the

**Table 4** The results of comparison between optimal and conventional engines

| Case | | $a_{max}$ (m/s$^2$) | Increase in $\varepsilon$ (%) | Decrease in $Q$ (%) | Decrease in $W_Q$ (%) | Decrease in $W_{f,\tau}$ (%) |
|---|---|---|---|---|---|---|
| Constrained acceleration | – | $5\times10^3$ | 0.31 | 7.85 | –3.83 | 4.35 |
| | – | $1\times10^4$ | 2.45 | 17.77 | 19.62 | 12.01 |
| | symmetric | $1\times10^4$ | 1.36 | 15.29 | 5.02 | 12.01 |
| | – | $2\times10^4$ | 4.59 | 23.14 | 29.90 | 12.31 |
| | – | $5\times10^4$ | 9.17 | 26.86 | 36.36 | 12.16 |
| Unconstrained acceleration | (1) | ∞ | 11.16 | 31.82 | 45.69 | 13.06 |
| | (2) | ∞ | 17.16 | 55.82 | 67.81 | –12.92 |
| | (3) | ∞ | 9.29 | –0.68 | 15.32 | 21.62 |
| | (4) | ∞ | 11.15 | 14.36 | 30.99 | 19.28 |
| | (5) | ∞ | 14.42 | 66.07 | 58.84 | 2.93 |

peak velocity for the optimal motion appears in this region (see Figures 2 and 3), and then the time spent on the contact between the working fluid and the cylinder wall in this region is relatively short. As a result, both $W_Q$ and $Q$ are decreased. Simultaneously, due to the higher temperature the heat saved here will be transformed into greater available work, which increases the effectiveness and the work per cycle, optimization has a much more remarkable effect on $W_Q$ than on $Q$. The changes of $T_f$ in Tables 2 and 3 show that the decrease in the heat leakage loss results in the increase in the final temperature $T_f$ on the power stroke. For the case (3) with unconstrained acceleration, a great portion of the increase in effectiveness is due to the decrease in the frictional loss $W_{f,\tau}$, and the reason is that the friction coefficient $\mu$ for this case is the largest. For all of the cases with unconstrained acceleration except the case (3) with the largest friction coefficient, the effectiveness $\varepsilon$ is improved by from 9.29% to 17.16%, the work lost due to the heat leakage ($W_Q$) is decreased by between 30.99% and 67.81%, but the relative decrease in the frictional loss $W_{f,\tau}$ never surpasses 21.62%. Especially for the case (2) with unconstrained acceleration, $\varepsilon$ is improved by 17.16% and $W_Q$ is decreased by 67.81%, but the frictional loss per cycle $W_{f,\tau}$ is decreased by 12.9%. It is evident that the increase in effectiveness is mainly due to the decrease in the heat leakage loss, and secondarily due to the decrease in the frictional loss. From Table 4, one can also see that for the optimal trajectories with $a_{max} > 1\times10^4$ m/s$^2$, there is little decrease in frictional loss, while the improvement in effectiveness is mainly due to the decrease in $W_Q$. For the maximum accelerations $1\times10^4$, $2\times10^4$ and $5\times10^4$ m/s$^2$, respectively, the corresponding effectiveness are improved by 2.45%, 4.59% and 9.1%, respectively, after optimizing the piston motion. Thus for the optimal trajectories with constrained acceleration, the effectiveness will be improved with the increase of the maximum acceleration, but the value of the improvement in effectiveness won't surpass 11.16%, which is the improvement for the case with unconstrained acceleration.

### 3.5 Comparison between the optimal piston motions with different heat transfer laws

Figure 5 shows the piston velocity versus the piston position on the power stroke for several different conditions, which include the purely sinusoidal motion, the modified sinusoidal motion and the optimal trajectory with unconstrained acceleration with linear phenomenological (this paper) and Newton's[22,23] heat transfer laws. Table 5 lists the corresponding results of numerical calculations. From Figure 5, the optimal trajectory with the linear phenomenological heat transfer law varies much compared to that with the Newton's heat transfer law, i.e. the relationship curve between the piston velocity and the piston position becomes much more smooth. In addition, from the results in Table 5, one can see that the optimal times $t_p$ spent on the power stroke with different heat transfer laws are different, i.e. the optimal distributions of the total cycle time $\tau$ among the strokes

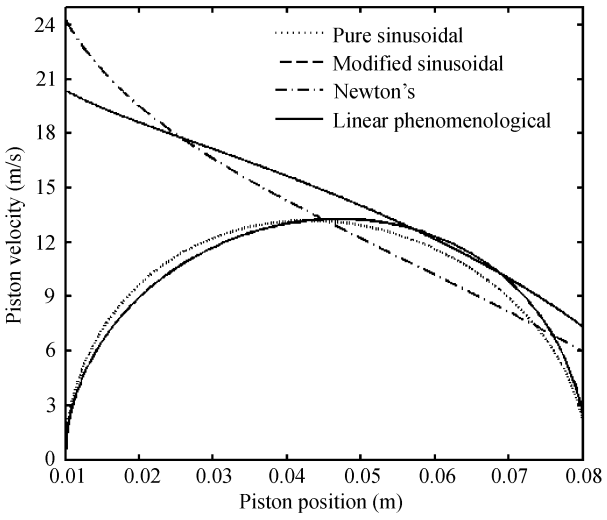


**Figure 5** Piston motions on the power stroke.

**Table 5** Numerical results for various piston motions with the Newton's and linear phenomenological heat transfer laws[a)]

| Case | | $v_{max}$ (m/s) | $t_p$ (ms) | $W_p$ (J) | $W_\tau$ (J) | $W_{f,\tau}$ (J) | $W_Q$ (J) | $Q$ (J) | $W_Q/Q$ | $T_f$ (K) | $\varepsilon$ |
|---|---|---|---|---|---|---|---|---|---|---|---|
| Newton's | pure-sin | 13.21 | 8.33 | 499.0 | 283.4 | 65.57 | 47.51 | 223.9 | 0.2122 | 1100 | 0.6502 |
| | modi-sin | 13.30 | 8.33 | 497.4 | 278.2 | 66.56 | 48.80 | 224.7 | 0.2172 | 1101 | 0.6382 |
| | opt. | 24.27 | 5.78 | 515.7 | 315.4 | 57.15 | 24.77 | 162.7 | 0.1522 | 1185 | 0.7235 |
| Linear phenomenological | pure-sin | 13.21 | 8.33 | 505.8 | 290.1 | 65.57 | 40.82 | 243.1 | 0.1679 | 1041 | 0.6656 |
| | modi-sin | 13.30 | 8.33 | 504.4 | 285.2 | 66.56 | 41.81 | 242.3 | 0.1725 | 1044 | 0.6543 |
| | opt. | 20.37 | 5.18 | 516.3 | 316.8 | 57.86 | 22.70 | 164.8 | 0.1377 | 1176 | 0.7267 |

a) Except $k$, other parameters are the same for the two heat transfer laws in calculations. For Newton's heat transfer law, $k = 1305$ W/(m$^2\cdot$K); for linear phenomenological heat transfer law, $k = 1.41\times10^9$ W$\cdot$K/m$^2$.

are distinct. Both the above two kinds of difference show that heat transfer law has important effects on the optimal piston trajectory.

There are two reasons for this difference. One is that the heat transfer laws are different, and the another is that the heat transfer coefficients change largely between different heat transfer laws. The similarities and differences for the optimal piston motions with different heat transfer laws are as follows: They both consist of three segments, including two boundary segments (maximum acceleration and maximum deceleration) and a middle movement segment; both the middle movement segment and corresponding optimal solution with unconstrained acceleration satisfy the same differential equations, so the differences of the optimal piston motion for unconstrained acceleration with different heat transfer laws bring on the differences of the optimal piston motion for constrained acceleration with different heat transfer laws. Compared to the optimal piston motion with the Newton's heat transfer law[22,23], the optimal piston motion for the whole cycle with the linear phenomenological heat transfer law has different optimal path on the power stroke and optimal distribution of the total cycle time among the strokes.

## 4 Conclusion

On the basis of refs. [22,23], this paper studies an Otto cycle engine with internal and external irreversibilities of friction and heat leakage, in which the heat transfer between the working fluid and the cylinder wall obeys the linear phenomenological heat transfer law. The optimal piston trajectory for maximizing the work per cycle is derived for the fixed total cycle time and fuel consumed per cycle. Optimal control theory is applied to determine the optimal piston trajectories for the cases of unconstrained and constrained piston accelerations on each stroke and the optimal distribution of the total cycle time among the strokes. The optimal piston motion with constrained acceleration on each stroke consists of three segments, including initial maximum acceleration and final maximum deceleration boundary segment, respectively, but the interior segment on the power stroke is different from those on the nonpower strokes. Numerical examples for the cases with unconstrained acceleration are given by using Matlab. The effects of changes of different parameters on the optimal configuration of piston motion are analyzed. The results show that optimizing the piston motion could improve engine power and efficiency by more than 9%, which is primarily due to the decrease of heat leakage loss on the initial portion of the power stroke. The obtained results are compared with those obtained with the Newton's heat transfer law[23]. It shows that heat transfer law influences the optimal configurations of piston motion, i.e. both the optimal path on the power stroke and optimal distribution of the total cycle time among the strokes are different for different heat transfer laws. For the case $a_{\max} = 2\times10^4$ m/s$^2$, the optimal piston trajectory for the whole cycle is shown in Figure 4. There are in fact several ways of achieving those pathways of which one points out just two: One mechanical solution is using a contoured plate to guide the piston on the desired path, and the other completely different way to transform the optimized paths is the use of an electrical coupling, see page 42 of ref. [2] in detail. Optimizing the piston motion not only improves the effectiveness and power, but also reduces the heat leakage and frictional loss. These have great significance for the design and operation of a real internal combustion engine. The decrease of the frictional loss results in the extension of the engine life. The decrease of heat leakage results in the decrease of the cooling demands; perhaps a simple air-cooling system could be used to substitute the complex liquid-cooling system. Besides, the exhaust gas temperature is higher for the optimized engine, and a heat accumulator may be used to restore the heat of the exhaust gas for secondary utilization. Optimizing the piston motion not only improves the power, effectiveness and operating conditions of the engine, but also decreases the investment and cost of the engine. This could provide some guidelines for the optimal design and operation of practical heat engines.

*The authors would like to thank Prof. Hoffman K H of Universitat Heidelberg in Germany for his suggestions on solving the optimal control problems.*

1 Andresen B, Berry R S, Ondrechen M J, et al. Thermodynamics for processes in finite time. Acc Chem Res, 1984, 17(8): 266－271

2 Sieniutycz S, Salamon P. Advances in Thermodynamics. Volume 4: Finite Time Thermodynamics and Thermoeconomics. New York: Taylor & Francis, 1990

3 Bejan A. Entropy generation minimization: The new thermodynamics of finite-size devices and finite-time processes. J Appl Phys, 1996, 79(3): 1191－1218

4 Berry R S, Kazakov V A, Sieniutycz S, et al. Thermodynamic Optimization of Finite Time Processes. Chichester: Wiley, 1999
5 Chen L, Wu C, Sun F. Finite time thermodynamic optimization or entropy generation minimization of energy systems. J Non-Equilib Thermodyn, 1999, 24(4): 327－359
6 Hoffman K H, Burzler J, Fischer A, et al. Optimal process paths for endoreversible systems. J Non-Equilib Thermodyn, 2003, 28(3): 233－268
7 Chen L, Sun F. Advances in Finite Time Thermodynamics: Analysis and Optimization. New York: Nova Science Publishers, 2004
8 Chen L. Finite Time Thermodynamic Analysis of Irreversible Progresses and Cycles (in Chinese). Beijing: High Education Press, 2005
9 Wang J, He J, Mao Z. Performance of quantum heat engine cycle with harmonic system. Sci China Ser G-Phys Mech Astron, 2007, 50(2): 163－176
10 Xia D, Chen L, Sun F. Optimal performance of a generalized irreversible four-reservoir isothermal chemical potential transformer. Sci China Ser B-Chem, 2008, 51(10): 958－970
11 Cutowicz-Krusin D, Procaccia J, Ross J. On the efficiency of rate process: Power and efficiency of heat engines. J Chem Phys, 1978, 69(9): 3898－3906
12 Curzon F L, Ahlborn B. Efficiency of a Carnot engine at maximum power output. Am J Phys, 1975, 43(1): 22－24
13 Rubin M H. Optimal configuration of a class of irreversible heat engines. Phys Rev A, 1979, 19(3): 1272－1287
14 Rubin M H. Optimal configuration of an irreversible heat engine with fixed compression ratio. Phys Rev A, 1980, 22(4): 1741－1752
15 Band Y B, Kafri O, Salamon P. Maximum work production from a heated gas in a cylinder with piston. Chem Phys Lett, 1980, 72(1): 127－130
16 Band Y B, Kafri O, Salamon P. Finite time thermodynamics: Optimal expansion of a heated working fluid. J Appl Phys, 1982, 53(1): 8－28
17 Band Y B, Kafri O, Salamon P. Optimization of a model external combustion engine. J Appl Phys, 1982, 53(1): 29－33
18 Salamon P, Band Y B, Kafri O. Maximum power from a cycling working fluid. J Appl Phys, 1982, 53(1): 197－202
19 Aizenbud B M, Band Y B. Power considerations in the operation of a piston fitted inside a cylinder containing a dynamically heated working fluid. J Appl Phys, 1981, 52(6): 3742－3744
20 Aizenbud B M, Band Y B, Kafri O. Optimization of a model internal combustion engine. J Appl Phys, 1982, 53(3): 1277－1282
21 Huleihil M, Andresen B. Optimal piston trajectories for adiabatic processes in the presence of friction. J Appl Phys, 2006, 100(11): 114914
22 Mozurkewich M, Berry R S. Finite-time thermodynamics: Engine performance improved by optimized piston motion. Proc Natl Acad Sci USA, 1981, 78(4): 1986－1988
23 Mozurkewich M, Berry R S. Optimal paths for thermodynamic systems. The ideal Otto cycle. J Appl Phys, 1982, 53(1): 34－42
24 Hoffman K H, Watowich S J, Berry R S. Optimal paths for thermodynamic systems. The ideal Diesel cycle. J Appl Phys, 1985, 58(6): 2125－2134
25 Blaudeck P, Hoffman K H. Optimization of the power output for the compression and power stroke of the Diesel engine. Proceedings of The International Conference ECOS'95, Istanbul, Turkey, 1995, Vol. 2: 754
26 De Vos A. Efficiency of some heat engines at maximum power conditions. Am J Phys, 1985, 53(6): 570－573
27 Chen L, Sun F, Wu C. The influence of heat transfer law on the endoreversible Carnot refrigerator. J Inst Energy, 1996, 69(479): 96－100
28 Chen L, Sun F, Wu C. Effect of heat transfer law on the performance of a generalized irreversible Carnot engine. J Phys D-Appl Phys, 1999, 32(2): 99－105
29 Chen L, Bi Y, Wu C. Unified description of endoreversible cycles for another linear heat transfer law. Int J Energy Environ Econ, 1999, 9(2): 77－93
30 Huleihil M, Andresen B. Convective heat transfer law for an endoreversible engine. J Appl Phys, 2006, 100(1): 014911
31 Qin X, Chen L, Sun F. Performance of real absorption heat-transformer with a generalized heat transfer law. Appl Thermal Eng, 2008, 28(7): 767－776
32 Qin X, Chen L, Sun F, et al. Model of real absorption heat pump cycle with a generalized heat transfer law and its performance. Proc Inst Mech Eng Part A-Power Energy, 2007, 221(A7): 907－916
33 Song H, Chen L, Li J, et al. Optimal configuration of a class of endoreversible heat engines with linear phenomenological heat transfer law. J Appl Phys, 2006, 100(12): 124907
34 Song H, Chen L, Sun F. Endoreversible heat engines for maximum power output with fixed duration and radiative heat-transfer law. Appl Energy, 2007, 84(4): 374－388
35 Song H, Chen L, Sun F. Optimal configuration of a class of endoreversible heat engines for maximum efficiency with radiative heat transfer law. Sci China Ser G-Phys Mech Astron, 2008, 51(9): 1272－1286
36 Chen L, Sun F, Wu C. Optimal expansion of a heated working fluid with phenomenological heat transfer. Energy Conv Manag, 1998, 39(3/4): 149－156
37 Song H, Chen L, Sun F. Optimal expansion of a heated working fluid for maximum work output with generalized radiative heat transfer law. J Appl Phys, 2007, 102(9): 094901
38 Burzler M J, Hoffman K H. Optimal Piston Paths for Diesel Engines. Chapter 7: Thermodynamics of energy conversion and transport. Sienuitycz S, de Vos A, eds. New York: Springer, 2000
39 Burzler J M. Performance optima for endoreversible systems. Doctor Dissertation. Chemnitz: University of Chemnitz, 2002
40 Taylor C F. The Internal Combustion Engine in Theory and Practice, Volumes 1 and 2. Cambridge, MA: The MIT Press, 1977
41 Biezeno C B, Grammel R. Engineering Dynamics, vol 4. London: Blackie, 1955. 2－5
42 Andresen B, Rubin M H, Berry R S. Availability for finite-time processes. General theory and a model. J Chem Phys, 1983, 87(15): 2704－2713